

Anion-Complexation-Induced Stabilization of Charge Separation

Francis D'Souza,^{*,†} Navaneetha K. Subbaiyan,[†] Yongshu Xie,^{‡,⊥} Jonathan P. Hill,^{*,‡}
Katsuhiko Ariga,[‡] Kei Ohkubo,[§] and Shunichi Fukuzumi^{*,§}

*Department of Chemistry, Wichita State University, 1845 Fairmount,
Wichita, Kansas 67260-0051, WPI Center for Materials Nanoarchitectonics (MANA), National
Institute for Materials Science, Namiki 1-1, Tsukuba, Ibaraki 305-0044, Japan, Key Laboratory for
Advanced Materials and Institute of Fine Chemicals, East China University of Science &
Technology, Shanghai 200237, P. R. China, and Graduate School of Engineering, Osaka University,
SORST (JST), Suita, Osaka 565-0871, Japan*

Received June 12, 2009; E-mail: Francis.DSouza@wichita.edu; Jonathan.Hill@nims.go.jp;
fukuzumi@chem.eng.osaka-u.ac.jp

Abstract: A supramolecular oligochromophoric system possessing exclusive binding sites for both a guest electron acceptor and an anionic cofactor species is developed, and anion-binding-induced stabilization of the charge-separated (CS) state is demonstrated. Toward this, intramolecular and intermolecular photochemical processes of a supramolecular complex of a bis-porphyrinyl-substituted oxoporphyrinogen with a bis(4-pyridyl)-substituted fullerene were investigated by using femtosecond and nanosecond laser flash photolysis measurements. Transient absorption spectra of the supramolecular complex obtained by femtosecond laser flash photolysis indicate that efficient electron transfer occurs from the porphyrin moiety to the fullerene moiety, followed by faster back electron transfer to the ground state. Binding of several different anionic species at the pyrrole amine groups of an oxoporphyrinogen unit within the supramolecular complex was found to improve the rate of the photoinduced electron transfer due to the favorable structural change. The anion binding also improves persistence of the photoinduced CS state between the anion-bound oxoporphyrinogen and fullerene moieties, which is produced by intermolecular electron transfer from the triplet excited state of free porphyrin molecules to free fullerene molecules, as indicated by the nanosecond laser flash photolysis measurements. In the case of fluoride anion binding, anion-complexation-induced stabilization of charge separation gave a 90-fold elongation of the CS state lifetime from 163 ns to 14 μ s. Complexation with other anions (acetate or dihydrogen phosphate) also resulted in stabilization of the CS state, whereas weakly bound perchlorate anions gave no improvement. Complexation of anions to the oxoporphyrinogen center lowers its oxidation potential by nearly 600 mV, creating an intermediate energy state for charge migration from the ZnP^{+} to the oxoporphyrinogen:anion complex. An increase in reorganizational energy of electron transfer combined with the decrease in charge recombination driving force caused by anion binding results in an increase in the lifetime of the CS state.

Introduction

Complex oligochromophoric molecular systems containing porphyrins are essential specimens for study of a variety of photoinduced reactions.¹ Thus, many chromophoric compounds have been prepared and analyzed for the lifetimes of their

charge-separated (CS) states,^{2–10} which have relevance to photosynthesis, or for their photonic applications.¹¹ Molecular donor–acceptor systems composed of tetrapyrroles (porphyrins) and electron acceptors such as fullerenes have attracted special attention.^{12–18} In certain cases, activity of naturally occurring systems is optimum only in the presence of an ionic cofactor either due to resulting structural stabilization¹⁹ or because of charge-balancing by the ion.²⁰ This situation can be referred to as “heterotropic allosteric regulation” and is observed in many enzyme systems using organic or inorganic ions. For example,

[†] Wichita State University.

[‡] National Institute for Materials Science.

[⊥] East China University of Science & Technology.

[§] Osaka University.

(1) (a) Gust, D.; Moore, T. A. In *The Porphyrin Handbook*; Kadish, K. M., Smith, K. M., Guillard, R., Eds.; Academic Press: New York, 2000; Vol. 8, pp 153–190. (b) Fukuzumi, S.; Imahori, H. In *Electron Transfer in Chemistry*; Balzani, V., Ed.; Wiley-VCH: Weinheim, 2001; Vol. 2, pp 927–975. (c) Chitta, R.; D'Souza, F. *J. Mater. Chem.* **2008**, *18*, 1440. (d) Paddon-Row, M. N. In *Stimulating Concepts in Chemistry*; Voegtle, F., Stoddart, J. F., Shibasaki, M., Eds.; Wiley-VCH: Weinheim, 2000; pp 267–291. (e) Saha, S.; Flood, A. H.; Stoddart, J. F.; Impellizzeri, S.; Silvi, S.; Venturi, M.; Credi, A. *J. Am. Chem. Soc.* **2007**, *129*, 12159. (f) Winters, M. U.; Kaernbratt, J.; Blades, H. E.; Frampton, M. J.; Anderson, H. L.; Albinsson, B. *Chem.—Eur. J.* **2007**, *13*, 7385. (g) Straight, S. D.; Andreasson, J.; Kodis, G.; Moore, A. L.; Moore, T. A.; Gust, D. *J. Am. Chem. Soc.* **2005**, *127*, 2717. (h) D'Souza, F.; Ito, O. *Chem. Commun.* **2009**, 4913.

(2) (a) Baranoff, E.; Barigelletti, F.; Bonnet, S.; Collin, J.-P.; Flamigni, L.; Mobian, P.; Sauvage, J.-P. In *Structure and Bonding*; Yam, V. W. W., Ed.; Springer: Berlin, 2007; Vol. 123, pp 41–78. (b) Paddon-Row, M. N. *Aust. J. Chem.* **2003**, *56*, 729. (c) Imahori, H.; Guldi, D. M.; Tamaki, K.; Yoshida, Y.; Luo, C.; Sakata, Y.; Fukuzumi, S. *J. Am. Chem. Soc.* **2001**, *123*, 6617. (d) Imahori, H.; Sekiguchi, Y.; Kashiwagi, Y.; Sato, T.; Araki, Y.; Ito, O.; Yamada, H.; Fukuzumi, S. *Chem.—Eur. J.* **2004**, *10*, 3184. (e) Kelley, R. F.; Shin, W. S.; Rybtchinski, B.; Sinks, L. E.; Wasielewski, M. R. *J. Am. Chem. Soc.* **2007**, *129*, 3173. (f) Kodis, G.; Terazono, Y.; Liddell, P. A.; Andréasson, J.; Garg, X.; Hamburger, M.; Moore, T. A.; Moore, A. L.; Gust, D. *J. Am. Chem. Soc.* **2006**, *128*, 1818.

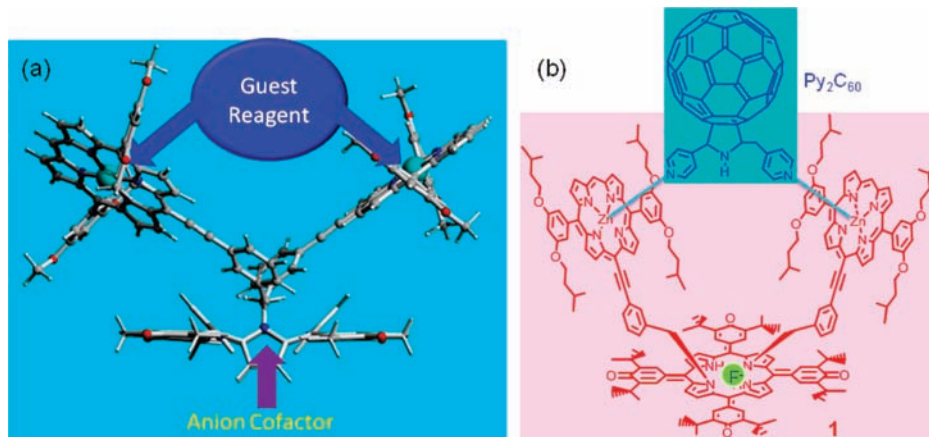


Figure 1. (a) Structural origin of two-guest reagent/anion cofactor complexation (peripheral substituents are omitted for clarity) and (b) chemical structure of the bis-porphyrin-substituted oxoporphyrinogen (**1**) and bis(4-pyridyl)-substituted fullerene used in this work. Axial coordination and anion binding site are also shown for clarity.

Nature uses chloride anions as a cofactor of the oxygen-evolving complex.^{21,22} In order to accommodate both reagent(s) and cofactor(s) in locations appropriate for their functions, it is necessary that a biological enzyme or synthetic species should possess at least two different binding sites.

Inspired by the above concept, here we have built a supramolecular oligochromophoric model system containing sites for binding of a reagent species and an anionic species in order to probe the effect of the binding of an anionic cofactor on the identities of products from photoinduced processes that occur within the resulting complex. This is important because investigation of the identity and stability of photoinduced CS complexes provides insights into methods for modulating potentially useful electronic properties of synthetic systems.

The concept of the dual binding mode of compound **1** is illustrated in Figure 1. The bis-porphyrin-substituted oxoporphyrinogen **1** (Figure 1b) has two different binding sites, as required. One site (composed of two porphinatozinc(II) units)

is capable of binding bis(4-pyridyl)-substituted guests through coordination to the central zinc cations,²³ while the other site (composed of two pyrrole-type amine groups of the oxoporphyrinogen unit) interacts with anionic species through hydrogen bonding.²⁴ The anion-binding site, the oxoporphyrinogen (OxP) unit, prepared by the two-electron oxidation of tetrakis(3,5-di-*tert*-butyl-4-hydroxyphenyl)porphyrin, can be multiply substi-

- (3) (a) Ajayaghosh, A.; Praveen, V. K.; Vijayakumar, C. *Chem. Soc. Rev.* **2008**, *37*, 109. (b) Eckert, J.-F.; Nicoud, J.-F.; Nierengarten, J.-F.; Liu, S.-G.; Echegoyen, L.; Barigelletti, F.; Armaroli, N.; Ouali, L.; Krasnikov, V.; Hadziioannou, G. *J. Am. Chem. Soc.* **2000**, *122*, 7467. (c) Beckers, E. H. A.; Meskers, S. C. J.; Schenning, A. P. H. J.; Chen, Z.; Wuerthner, F.; Janssen, R. A. J. *J. Phys. Chem. A* **2004**, *108*, 6933. (d) Giacalone, F.; Segura, J. L.; Martin, N.; Ramey, J.; Guldi, D. M. *Chem.—Eur. J.* **2005**, *11*, 4819. (e) Burquel, A.; Lemaure, V.; Beljonne, D.; Lazzaroni, R.; Cornil, J. *J. Phys. Chem. A* **2006**, *110*, 3447. (f) Neuteboom, E. E.; Meskers, S. C. J.; Van Hal, P. A.; Van Duren, J. K. J.; Meijer, E. W.; Janssen, R. A. J.; Dupin, H.; Pourtois, G.; Cornil, J.; Lazzaroni, R.; Bredas, J.-L.; Beljonne, D. *J. Am. Chem. Soc.* **2003**, *125*, 8625. (g) Figueira-Duarte, T. M.; Rio, Y.; Listorti, A.; Delavaux-Nicot, B.; Holler, M.; Marchioni, F.; Ceroni, P.; Armaroli, N.; Nierengarten, J.-F. *New J. Chem.* **2008**, *32*, 54.
- (4) (a) Savova, G. H.; Hartnagel, U.; Balbinot, D.; Sali, S.; Jux, N.; Hirsh, A.; Guldi, D. M. *Chem.—Eur. J.* **2008**, *14*, 3137. (b) de la Escosura, A.; Martínez-Díaz, M. V.; Guldi, D. M.; Torres, T. *J. Am. Chem. Soc.* **2006**, *128*, 4112. (c) Guldi, D. M.; Gouloumis, A.; Vázquez, P.; Torres, T.; Georgakilas, V.; Prato, M. *J. Am. Chem. Soc.* **2005**, *127*, 5811. (d) Ohkubo, K.; Fukuzumi, S. *J. Porphyrins Phthalocyanines* **2008**, *12*, 993. (e) Ohkubo, K.; Fukuzumi, S. *Bull. Chem. Soc. Jpn.* **2009**, *82*, 303. (f) Jimenez, A. J.; Spaenig, F.; Rodriguez-Morgade, M. S.; Ohkubo, K.; Fukuzumi, S.; Guldi, D. M.; Torres, T. *Org. Lett.* **2007**, *9*, 2481. (g) Gouloumis, A.; de la Escosura, A.; Vázquez, P.; Torres, T.; Kahnt, A.; Guldi, D. M.; Neugebauer, H.; Winder, C.; Drees, M.; Sariciftci, N. S. *Org. Lett.* **2006**, *8*, 5187. (h) Li, L.; Shen, S.; Yu, Q.; Zhou, Q.; Xu, H. *J. Chem. Soc., Chem. Commun.* **1991**, *9*, 619. (i) Marino-Ochoa, E.; Palacios, R.; Kodis, G.; Macpherson, A. N.; Gillbro, T.; Gust, D.; Moore, T. A.; Moore, A. L. *Photochem. Photobiol.* **2002**, *76*, 116.
- (5) (a) Hauschild, R.; Riedel, G.; Zeller, J.; Balaban, T. S.; Prokhorenko, V. I.; Kalt, H.; Berova, N.; Huang, X.; Pescitelli, R.; Nakanishi, K. *J. Lumin.* **2005**, *112*, 454. (b) Balaban, T. S.; Bhise, A. D.; Fischer, M.; Linke-Schaetzl, M.; Roussel, C.; Vanthuyne, N. *Angew. Chem., Int. Ed.* **2003**, *42*, 2139. (c) Balaban, T. S. Light-harvesting Nanostructures. In *Encyclopedia of Nanoscience and Nanotechnology*; Nalwa, H. S., Ed.; American Scientific Publishers: Los Angeles, 2004; Vol. 4, pp 505–559.
- (6) (a) Schumacher, A. L.; Sandanayaka, A. S. D.; Hill, J. P.; Ariga, K.; Karr, P. A.; Araki, Y.; Ito, O.; D'Souza, F. *Chem.—Eur. J.* **2007**, *13*, 4628. (b) Hill, J. P.; Sandanayaka, A. S. D.; McCarty, A. L.; Karr, P. A.; Zandler, M. E.; Charvet, R.; Ariga, K.; Araki, Y.; Ito, O.; D'Souza, F. *Eur. J. Org. Chem.* **2006**, 595.
- (7) (a) Choi, M.-S.; Yamazaki, T.; Yamazaki, I.; Aida, T. *Angew. Chem., Int. Ed.* **2004**, *43*, 150. (b) Choi, M.-S.; Aida, T.; Yamazaki, T.; Yamazaki, I. *Chem.—Eur. J.* **2002**, *8*, 2667.
- (8) (a) Rybtchinski, B.; Sinks, L. E.; Wasielewski, M. R. *J. Am. Chem. Soc.* **2004**, *126*, 12268. (b) van der Boom, T.; Hayes, R. T.; Zhao, Y.; Bushard, P. J.; Weiss, E. A.; Wasielewski, M. R. *J. Am. Chem. Soc.* **2002**, *124*, 9582. (c) Lukas, A. S.; Zhao, Y.; Miller, S. E.; Wasielewski, M. R. *J. Phys. Chem. B* **2002**, *106*, 1299. (d) Ghirotti, M.; Chiorboli, C.; You, C.-C.; Wuerthner, F.; Scandola, F. *J. Phys. Chem. A* **2008**, *112*, 3376. (e) Flamigni, L.; Ventura, B.; You, C.-C.; Hippus, C.; Wuerthner, F. *J. Phys. Chem. C* **2007**, *111*, 622.
- (9) (a) Oseki, Y.; Fujitsuka, M.; Cho, D. W.; Sugimoto, A.; Tojo, S.; Majima, T. *J. Phys. Chem. B* **2005**, *109*, 19257. (b) Nakamura, T.; Ikemoto, J.; Fujitsuka, M.; Araki, Y.; Ito, O.; Takimiya, K.; Aso, Y.; Otsubo, T. *J. Phys. Chem. B* **2005**, *109*, 14365. (c) van Hal, P. A.; Janssen, R. A. J.; Lanzani, G.; Cerullo, G.; Zavelani-Rossi, M.; De Silvestri, S. *Chem. Phys. Lett.* **2001**, *345*, 33.
- (10) (a) Li, K.; Bracher, P. J.; Guldi, D. M.; Herranz, M. A.; Echegoyen, L.; Schuster, D. I. *J. Am. Chem. Soc.* **2004**, *126*, 9156. (b) Schuster, D. I.; Cheng, P.; Jarowski, P. D.; Guldi, D. M.; Luo, C.; Echegoyen, L.; Pyo, S.; Holzwarth, A. R.; Braslavsky, S. E.; Williams, R. M.; Klich, G. *J. Am. Chem. Soc.* **2004**, *126*, 7257. (c) Montforts, F.-P.; Vlasiouk, I.; Smirnov, S.; Wedel, M. *J. Porphyrins Phthalocyanines* **2003**, *7*, 651. (d) Armaroli, N.; Diederich, F.; Dietrich-Buchecker, C. O.; Flamigni, L.; Marconi, G.; Nierengarten, J.-F.; Sauvage, J.-P. *Chem.—Eur. J.* **1998**, *4*, 406. (e) Sanchez, L.; Perez, I.; Martin, N.; Guldi, D. M. *Chem.—Eur. J.* **2003**, *9*, 2457. (f) Segura, J. L.; Priego, E. M.; Martin, N.; Luo, C.; Guldi, D. M. *Org. Lett.* **2000**, *2*, 4021.
- (11) (a) Fukuzumi, S. *Eur. J. Inorg. Chem.* **2008**, 1351. (b) Fukuzumi, S. *Phys. Chem. Chem. Phys.* **2008**, *10*, 2283. (c) Fukuzumi, S.; Kojima, T. *J. Mater. Chem.* **2008**, *18*, 1427. (d) Fukuzumi, S. *Bull. Chem. Soc. Jpn.* **2006**, *79*, 177. (e) Ohkubo, K.; Fukuzumi, S. *Bull. Chem. Soc. Jpn.* **2009**, *82*, 303.

tuted at central nitrogen atoms in a stepwise and regioselective way, permitting the synthesis of **1**.²⁵

The effect of anion binding on the intramolecular photoinduced electron-transfer processes was probed by using femto-second and nanosecond laser flash photolysis measurements of the supramolecular complex between **1** and Py₂C₆₀ in the absence and presence of different anions. As demonstrated, complexation of anions to the oxoporphyrinogen center lowers its oxidation potential by nearly 600 mV, creating an intermediate energy state for charge migration from the ZnP⁺ to the oxoporphyrinogen:anion complex. A decrease in charge recombination (CR) driving force caused by anion binding combined with an increase in reorganizational energy of electron transfer results in the desired increase in the lifetime of the CS state. The present study provides valuable insight into the role of anion binding on the control of the photodynamics of both photoinduced electron transfer and charge recombination reactions.

Experimental Section

Chemicals. Buckminsterfullerene, C₆₀ (+99.95%), was from SES Research, (Houston, TX). All the reagents were from Aldrich

Chemicals (Milwaukee, WI), while the bulk solvents utilized in the syntheses were from Fischer Chemicals. The tetra-*n*-butylammonium anion salts (*n*-Bu₄N)ClO₄ used in electrochemical and anion-binding studies were from Fluka Chemicals. The syntheses of OxP-(ZnP)₂, **1**, and fullerene were carried out according to our earlier published methods.^{23,26}

Instrumentation. ¹H NMR spectra were obtained from chloroform-*d* solutions using a JEOL 300 MHz NMR spectrometer with tetramethylsilane as an internal standard. The UV–visible spectral measurements were carried out with a Shimadzu model 1600 UV–visible spectrophotometer. The fluorescence emission was monitored by using a Varian Eclipse spectrometer. Cyclic voltammograms were recorded on a EG&G PARSTAT electrochemical analyzer using a three-electrode system. A platinum button electrode was used as the working electrode. A platinum wire served as the counter electrode, and an Ag/AgCl was used as the reference electrode. Ferrocene/ferricenium redox couple was used as an internal standard. All the solutions were purged prior to electrochemical and spectral measurements using argon gas.

Time-Resolved Transient Absorption Measurements. Femto-second laser flash photolysis was conducted using a Clark-MXR 2010 laser system and an optical detection system provided by Ultrafast Systems (Helios). The source for the pump and probe pulses was derived from the fundamental output of Clark laser system (775 nm, 1 mJ/pulse and fwhm = 150 fs) at a repetition rate of 1 kHz. A second harmonic generator introduced in the path of the laser beam provided 410 nm laser pulses for excitation. Of the fundamental output of the laser, 95% was used to generate the second harmonic; the remaining 5% of the deflected output was used for white light generation. Prior to generating the probe continuum, the laser pulse was fed to a delay line that provided an experimental time window of 1.6 ns with a maximum step resolution of 7 fs. The pump beam was attenuated at 5 μJ/pulse with a spot size of 2 mm diameter at the sample cell, where it was merged with the white probe pulse at a close angle (<10°). The probe beam, after passing through the 2 mm sample cell, was focused on a 200 μm fiber optic cable which was connected to a CCD spectrograph (Ocean Optics, S2000-UV-vis for visible region and Horiba, CP-140 for NIR region) for recording the time-resolved spectra (450–800 and 800–1400 nm). Typically, 5000 excitation pulses were averaged to obtain the transient spectrum at a set delay time.

- (12) (a) Schuster, D. I.; Li, K.; Guldi, D. M. *C. R. Chim.* **2006**, *9*, 892. (b) Guldi, D. M. *Chem. Soc. Rev.* **2002**, *31*, 22. (c) Imahori, H.; Sakata, Y. *Eur. J. Org. Chem.* **1999**, *10*, 2445. (d) Guldi, D. M.; Rahman, G. M.; Aminur, S. V.; Ehli, C. *Chem. Soc. Rev.* **2006**, *35*, 471. (e) Guldi, D. M.; Rahman, G. M. A.; Zerbetto, F.; Prato, M. *Acc. Chem. Res.* **2005**, *38*, 871. (f) Martini, N.; Sánchez, L.; Herranz, M. A.; Illescas, B.; Guldi, D. M. *Acc. Chem. Res.* **2007**, *40*, 1015.
- (13) (a) Isosomppi, M.; Tkachenko, N. V.; Efimov, A.; Lemmetyinen, H. *J. Phys. Chem. A* **2005**, *109*, 4881. (b) Vail, S. A.; Schuster, D. I.; Guldi, D. M.; Isosomppi, M.; Tkachenko, N.; Lemmetyinen, H.; Palkar, A.; Echegoyen, L.; Chen, X.; Zhang, J. Z. H. *J. Phys. Chem. B* **2006**, *110*, 14155. (c) Kaunisto, K.; Chukharev, V.; Tkachenko, N. V.; Efimov, A.; Lemmetyinen, H. *J. Phys. Chem. C* **2009**, *113*, 3819. (d) Schuster, D. I.; Li, K.; Guldi, D. M.; Palkar, A.; Echegoyen, L.; Stanisky, C.; Cross, R. J.; Niemi, M.; Tkachenko, N. V.; Lemmetyinen, H. *J. Am. Chem. Soc.* **2007**, *129*, 15973.
- (14) (a) Kuramochi, Y.; Sandanayaka, A. S. D.; Satake, A.; Araki, Y.; Ogawa, K.; Ito, O.; Kobuke, Y. *Chem.—Eur. J.* **2009**, *15*, 2317. (b) Kuramochi, Y.; Satake, A.; Itou, M.; Ogawa, K.; Araki, Y.; Ito, O.; Kobuke, Y. *Chem.—Eur. J.* **2008**, *14*, 2827–2841.
- (15) (a) Charvet, R.; Jiang, D.-L.; Aida, T. *Chem. Commun.* **2004**, 2664. (b) Luo, H.; Choi, M.-S.; Araki, Y.; Ito, O.; Aida, T. *Bull. Chem. Soc. Jpn.* **2005**, *78*, 405. (c) Choi, M.-S.; Aida, T.; Luo, H.; Araki, Y.; Ito, O. *Angew. Chem., Int. Ed.* **2003**, *42*, 4060.
- (16) (a) Balbinot, D.; Atalick, S.; Guldi, D. M.; Hatzimarinaki, M.; Hirsch, A.; Jux, N. *J. Phys. Chem. B* **2003**, *107*, 13273. (b) Milanese, M. E.; Gervald, M.; Otero, L. A.; Sereno, L.; Silber, J. J.; Durantini, E. N. *J. Phys. Org. Chem.* **2002**, *15*, 844. (c) Fungo, F.; Otero, L.; Borsarelli, C. D.; Durantini, E. N.; Silber, J. J.; Sereno, L. *J. Phys. Chem. B* **2002**, *106*, 4070. (d) Bell, T. D. M.; Smith, T. A.; Ghiggino, K. P.; Ranasinghe, M. G.; Shepard, M. J.; Paddon-Row, M. *Chem. Phys. Lett.* **1997**, *268*, 223.
- (17) (a) Xiao, S.; Li, Y.; Li, Y.; Zhuang, J.; Wang, N.; Liu, H.; Ning, B.; Liu, Y.; Lu, F.; Fan, L.; Yang, C.; Li, Y.; Zhu, D. *J. Phys. Chem. B* **2004**, *108*, 16677. (b) Lu, F.; Xiao, S.; Li, Y.; Liu, H.; Li, H.; Zhuang, J.; Liu, Y.; Wang, N.; He, X.; Li, X.; Gan, L.; Zhu, D. *Macromolecules* **2004**, *37*, 7444.
- (18) (a) Liddell, P. A.; Kuciauskas, D.; Sumida, J. P.; Nash, B.; Nguyen, D.; Moore, A. L.; Moore, T. A.; Gust, D. *J. Am. Chem. Soc.* **1997**, *119*, 1400. (b) Kuciauskas, D.; Lin, S.; Seely, G. R.; Moore, A. L.; Moore, T. A.; Gust, D.; Drovetzkaya, T.; Reed, C. A.; Boyd, P. D. W. *J. Phys. Chem.* **1996**, *100*, 15926. (c) Kuciauskas, D.; Liddell, P. A.; Lin, S.; Stone, S. G.; Moore, A. L.; Moore, T. A.; Gust, D. *J. Phys. Chem. B* **2000**, *104*, 4307. (d) Smirnov, S. N.; Liddell, P. A.; Vlassiuk, I. V.; Teslja, A.; Kuciauskas, D.; Braun, C. L.; Moore, A. L.; Moore, T. A.; Gust, D. *J. Phys. Chem. A* **2003**, *107*, 7567.
- (19) (a) Sessler, J. L.; Gale, P. A.; Cho, W.-S. *Anion Receptor Chemistry*; Royal Society of Chemistry: Cambridge, UK, 2006. (b) Burkhard, P.; Tai, C.-H.; Jansonius, J. N.; Cook, P. F. *J. Mol. Biol.* **2000**, *303*, 279. (c) Gossas, T.; Danielson, H. *Biochem. J.* **2006**, *398*, 393. (d) Zak, O.; Ikuta, K.; Aisen, P. *Biochemistry* **2002**, *41*, 7416. (e) Popelkova, H.; Commet, A.; Kuntzleman, T.; Yocum, C. F. *Biochemistry* **2008**, *47*, 12593.
- (20) (a) Siegbahn, P. E. M.; Crabtree, R. H. *J. Am. Chem. Soc.* **1999**, *121*, 117. (b) Jou, R.; Cowan, J. A. *J. Am. Chem. Soc.* **1991**, *113*, 6685. (c) Sessler, J. L.; Gale, P. A. In *The Porphyrin Handbook*; Kadish, K. M., Smith, K. M., Guillard, R., Eds.; Academic Press: San Diego, CA, 2000; Vol. 6, pp 257–258.
- (21) (a) Guskov, A.; Kern, J.; Gabdulkhakov, A.; Broser, M.; Zouni, A.; Saenger, W. *Nat. Struct. Mol. Biol.* **2009**, *16*, 334. (b) Barber, J. *Q. Rev. Biophys.* **2003**, *36*, 71. (c) van Gorkom, H. J.; Yocum, C. F. In *Photosystem II: the light-driven water: plastoquinone oxidoreductase*; Wydrzynski, T. J., Satoh, K., Eds.; Springer: Dordrecht, 2005; pp 307–328.
- (22) (a) Lindberg, K.; Vänngård, T.; Andréasson, L.-E. *Photosynth. Res.* **1993**, *38*, 401. (b) Wincencjusz, H.; Yocum, C. F.; van Gorkom, H. J. *Biochemistry* **1999**, *38*, 3719. (c) Popelkova, H.; Yocum, C. F. *Photosynth. Res.* **2007**, *93*, 111. (d) Guskov, A.; Kern, J.; Gabdulkhadov, A.; Broser, M.; Zouni, A.; Saenger, W. *Nature Struct. Mol. Biol.* **2009**, *16*, 334–342. (e) Murray, J. W.; Maghlaoui, K.; Kargul, J.; Ishida, N.; Lai, T.-L.; Rutherford, A. W.; Sugiura, M.; Bousgal, A.; Barber, J. *Energy Environ. Sci.* **2008**, *1*, 161–166. (f) Yocum, C. F. *Coord. Chem. Rev.* **2008**, *252*, 296–305.
- (23) Xie, Y.; Hill, J. P.; Schumacher, A. L.; Sandanayaka, A. S. D.; Araki, Y.; Karr, P. A.; Labuta, J.; D'Souza, F.; Ito, O.; Anson, C. E.; Powell, A. K.; Ariga, K. *J. Phys. Chem. C* **2008**, *112*, 10559.
- (24) Hill, J. P.; Schumacher, A. L.; D'Souza, F.; Labuta, J.; Redshaw, C.; Elsegood, M. R. J.; Aoyagi, M.; Nakanishi, T.; Ariga, K. *Inorg. Chem.* **2006**, *45*, 8288.
- (25) (a) Hill, J. P.; Hewitt, I. J.; Anson, C. E.; Powell, A. K.; McCarty, A. L.; Karr, P. A.; Zandler, M. E.; D'Souza, F. *J. Org. Chem.* **2004**, *69*, 5861. (b) Hill, J. P.; Schmitt, W.; McCarty, A. L.; Ariga, K.; D'Souza, F. *Eur. J. Org. Chem.* **2005**, 2893.
- (26) D'Souza, F.; Gadde, S.; Zandler, M. E.; Itou, M.; Araki, Y.; Ito, O. *Chem. Commun.* **2004**, 2276.

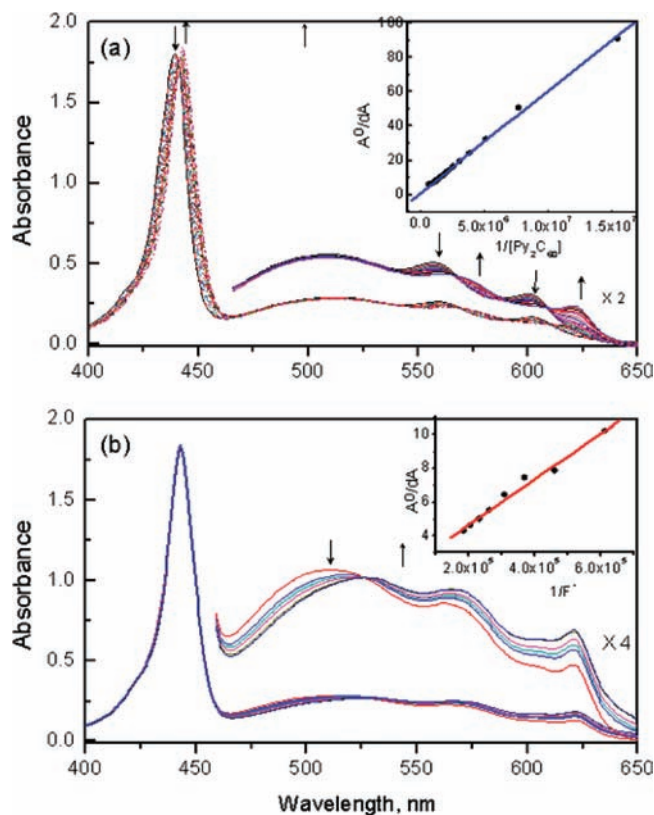


Figure 2. Optical absorption spectral changes observed during (a) binding of Py_2C_{60} to **1** to form the $1 \cdot \text{Py}_2\text{C}_{60}$ complex and (b) F^- binding to OxP of the $1 \cdot \text{Py}_2\text{C}_{60}$ complex to form the $1(\text{F}^-) \cdot \text{Py}_2\text{C}_{60}$ complex in *o*-dichlorobenzene. The figure insets show Benesi–Hildebrand plots constructed to obtain the binding constants; A° and dA represent respectively absorbance values in the absence of added guest and change in absorbance upon guest binding.

The kinetic traces at appropriate wavelengths were assembled from the time-resolved spectral data.

Nanosecond time-resolved transient absorption measurements were carried out using the laser system provided by UNISOKU Co., Ltd. Measurements of nanosecond transient absorption spectra were performed according to the following procedure. A deaerated solution containing a dyad was excited by a Panther optical parametric oscillator pumped by a Nd:YAG laser (Continuum, SLII-10, 4–6 ns fwhm) at $\lambda = 430$ nm. The photodynamics were monitored by continuous exposure to a xenon lamp (150 W) as a probe light and a photomultiplier tube (Hamamatsu 2949) as a detector. Transient spectra were recorded using fresh solutions in each laser excitation. The solution was deoxygenated by argon purging for 15 min prior to measurements.

Results and Discussion

Formation and Characterization of the Two-Guest Bound Supramolecular Host Complex. The formation of the two-guest bound supramolecular host system was followed in two steps, viz., Py_2C_{60} binding to the host system, **1**, to form $1 \cdot \text{Py}_2\text{C}_{60}$, and binding of anion to the OxP anion binding site to yield the $1(\text{F}^-) \cdot \text{Py}_2\text{C}_{60}$ supramolecular complex. Optical absorption and ^1H NMR studies were systematically performed to arrive at the stoichiometry and binding constants of the two-guest bound complex. Electronic spectral changes during binding of Py_2C_{60} to **1** are shown in Figure 2a. These spectra illustrate complexation of Py_2C_{60} with zinc porphyrin²⁶ as revealed by the red shift of absorbance bands of porphyrinatozinc of **1** located at 439, 513, and 601 nm to 443, 571, and 621 nm, respectively. The

Table 1. Binding Constants (K), Rate Constants of Charge Separation (k_{CS}^{S}) and Charge Recombination (k_{CR}^{T}), and Lifetimes of CS States (τ_{RIP}) for the Investigated Supramolecular Complexes in *o*-Dichlorobenzene

compound ^a	K (M^{-1})	k_{CS}^{S} (s^{-1})	k_{CR}^{T} (s^{-1})	τ_{RIP} (μs)
1 + Py_2C_{60}	1.9×10^5	1.6×10^{10}	6.1×10^6	0.16
1 : Py_2C_{60} + F^-	7.4×10^4	2.9×10^{10}	7.1×10^5	14
1 : Py_2C_{60} + CH_3COO^-	6.1×10^4	1.2×10^{10}	9.1×10^5	11
1 : Py_2C_{60} + H_2PO_4^-	8.4×10^2	1.5×10^{10}	1.3×10^5	7.5
1 : Py_2C_{60} + ClO_4^-	no binding	1.7×10^{10}	5.8×10^6	0.17

^a See Figure 1 for structures.

unique topology of **1** with a V-alignment of the porphyrin macrocycles allowed supramolecular complex formation by adopting the well-established “two-point” coordinative binding of bis-pyridine-functionalized fullerene.²³ The binding constant calculated using the Benesi–Hildebrand method²⁷ was $1.9 \times 10^5 \text{ M}^{-1}$ (Figure 1a inset). This value is nearly 2 orders of magnitude higher compared that that for mono-pyridine fulleropyrrolidine binding to zinc porphyrin,²⁸ mainly due to the cooperative effect induced by the bis-pyridine-functionalized fullerene to appropriately positioned zinc porphyrin macrocycles.^{23,26} A Job’s plot confirms 1:1 stoichiometry of the $1 \cdot \text{Py}_2\text{C}_{60}$ complex. It is important to note that the oxoporphyrinogen band located at 513 nm exhibited no shift in the band position, suggesting lack of direct interaction with ZnP or Py_2C_{60} . It may also be mentioned here that the geometry of $1 \cdot \text{Py}_2\text{C}_{60}$ deduced from the B3LYP/3-21G(*) method yielded a stable structure on the Born–Oppenheimer potential energy surface.²³

Anion binding to the OxP anion binding site was subsequently performed as shown for F^- binding to the $1 \cdot \text{Py}_2\text{C}_{60}$ complex in Figure 2b. The fluoride anion binding to the oxoporphyrinogen is indicated by the red shift of its absorbance band from 513 to 530 nm.²⁴ Notably, no further shifts of the porphyrin absorbance bands occur on addition of fluoride anions to a solution of the $1 \cdot \text{Py}_2\text{C}_{60}$ complex, indicating that fluoride anions do not interact with the porphyrinatozinc entities. This is due in part to the preferential binding of F^- to OxP as revealed by the higher K values and strong binding of Py_2C_{60} to the porphyrinatozinc moieties through the two-point binding motif,²³ which maintains the guest exclusivity of the two binding sites. The binding constant was calculated to be $7.4 \times 10^4 \text{ M}^{-1}$ (Figure 2b inset), and the molecular stoichiometry from the Job’s plot was found to be 1 equiv of F^- binding to the OxP pocket of the $1 \cdot \text{Py}_2\text{C}_{60}$ complex. Similar spectral changes were observed for acetate and dihydrogen phosphate binding to **1** (see Figures S1 and S2 in the Supporting Information for spectral changes and Benesi–Hildebrand plots); the binding constants are given in Table 1. Addition of ClO_4^- to the $1 \cdot \text{Py}_2\text{C}_{60}$ complex solution caused no detectable spectral changes, suggesting little or no binding of this anion to the OxP (Figure S3 in the Supporting Information). The anion binding constants are the same order of magnitude as the earlier reported values for anion binding to bis-benzyl OxP (ZnP entities replaced with benzyl groups), abbreviated as Ox(bz)₂.²⁴ Binding constants of the bis(4-pyridyl)fullerene guest to host **1** represent the binding of the mixture of diastereomers obtained during synthesis of Py_2C_{60} . The minor differences in geometry introduced to the host–guest complexes were consequently neglected.

(27) Benesi, H. A.; Hildebrand, J. H. *J. Am. Chem. Soc.* **1949**, *71*, 2703.

(28) D’Souza, F.; Deviprasad, G. R.; Zandler, M. E.; Hoang, V. T.; Arkady, K.; VanStipdonk, M.; Perera, A.; El-Khouly, M. E.; Fujitsuka, M.; Ito, O. *J. Phys. Chem. A* **2002**, *106*, 3243.

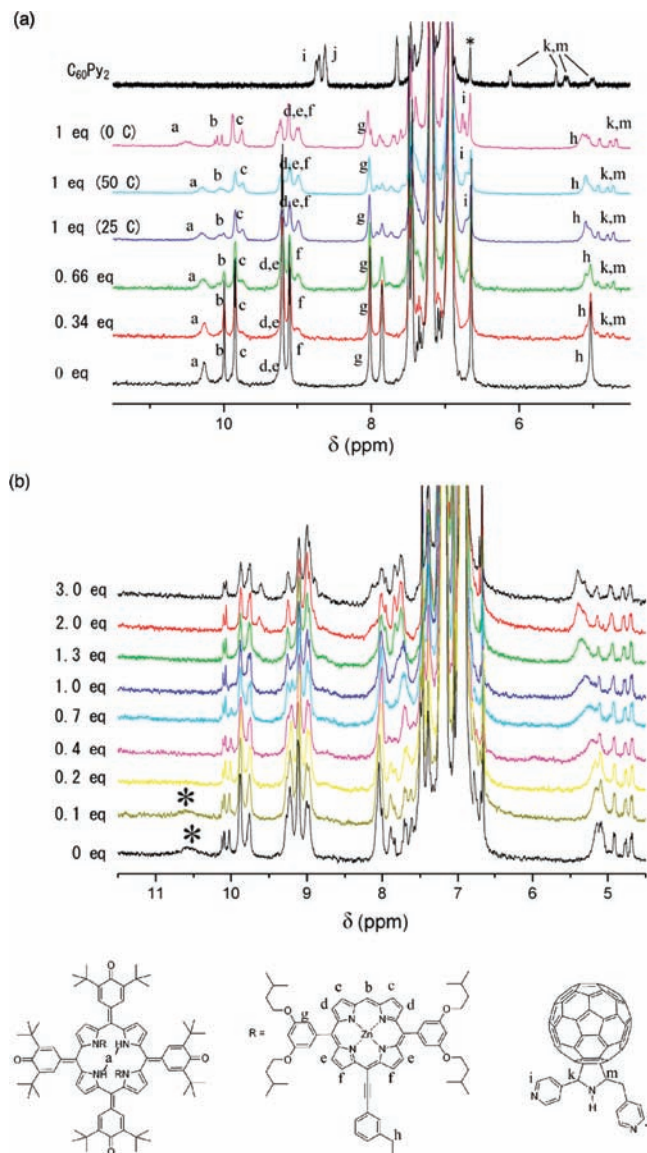


Figure 3. (a) ^1H NMR titration of **1** with up to 1 equiv of Py_2C_{60} in *o*-dichlorobenzene- d_4 . Note the upfield shift of resonances of Py_2C_{60} due to shielding by the porphyrin aromatic π -electronic system. Assignments of relevant peaks are shown in the lower part of the figure. (b) Titration of the $1\cdot\text{Py}_2\text{C}_{60}$ complex formed in (a) with fluoride anions (tetra-*n*-butylammonium fluoride solution in *o*-dichlorobenzene- d_4). Asterisk denotes porphyrinogen NH resonance. Note the disappearance of the peak labeled with an asterisk due to hydrogen bonding to fluoride anions.

Further evidence for the structure of the F^- -bound $1\cdot\text{Py}_2\text{C}_{60}$ complex was obtained by using ^1H NMR spectroscopy (see Figure 3). ^1H NMR spectra of **1** revealed gradual spectral changes during titration with up to 1 equiv of Py_2C_{60} in *o*-dichlorobenzene- d_4 (Figure 3a). That is, the resonances due to the axially coordinated pyridyl protons experienced an upfield shift (of around 2 ppm) as a result of their proximity to the porphyrin aromatic system, while shifts in the frequency of the resonances due to the ZnP or OxP entities were minimal. Addition of Py_2C_{60} beyond 1 equiv resulted in a gradual shift of the pyridyl proton resonances to their expected position due to exchange, suggesting a 1:1 stoichiometry for the $1\cdot\text{Py}_2\text{C}_{60}$ complex.

The complex appears to be stable even at 50 °C. Subsequent addition of 1 equiv of F^- to the solution of $1\cdot\text{Py}_2\text{C}_{60}$ resulted in the disappearance of the broad peak due to the NH protons

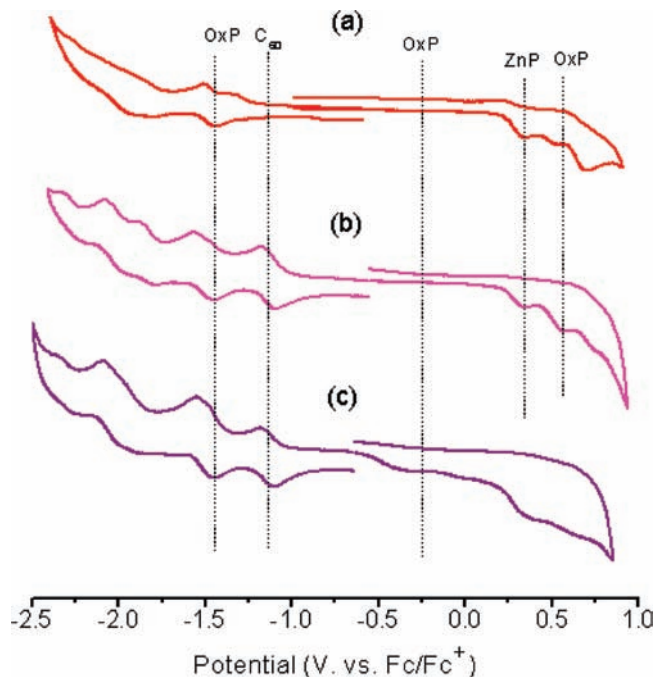


Figure 4. Cyclic voltammograms of (a) **1**, (b) $1\cdot\text{Py}_2\text{C}_{60}$ obtained from an equimolar mixture of **1** and Py_2C_{60} , and (c) $1(\text{F}^-)\cdot\text{Py}_2\text{C}_{60}$ obtained from an equimolar mixture of $1\cdot\text{Py}_2\text{C}_{60}$ and F^- . All measurements were performed in *o*-dichlorobenzene containing 0.1 M (*n*- Bu_4N) PF_6 . Scan rate, 100 mV/s. (*n*- Bu_4N) F was used as fluoride anion source.

of OxP (see Figure 3b), indicating F^- binding at the OxP anion binding site. The fullerene complexation appears not to be affected, even in the presence of up to 4 equiv of fluoride anions. These results, along with the earlier discussed optical absorption studies, prove the structural integrity of the supramolecular complex depicted in Figure 1.

Electrochemical Studies. Cyclic voltammetry studies were performed to evaluate the redox potentials of the individual entities and that of the supramolecular complex to estimate the free-energy change associated with the photoinduced electron-transfer events. As reported earlier, OxP and its *N*-substituted derivatives possess extended π -conjugation with four hemiquinone substituents at their peripheries; therefore, it is expected to undergo facile oxidation and reduction processes.²⁵ Furthermore, the redox-active *N*-substituents are expected to influence the redox potentials of the OxP core in addition to exhibiting their own redox processes. As shown in Figure S4a in the Supporting Information, the first oxidation and first reduction processes of OxP(bz)₂ occur at 0.48 and -1.37 V, respectively, vs Fc/Fc^+ . Replacing the *N*-benzyl substituents with zinc porphyrin entities leads to the appearance of additional redox processes corresponding to the ZnP entities (Figure 4a). The first oxidation involving ZnP is located at 0.28 V, while the first reduction involving the electron-deficient OxP macrocycle is located at -1.37 V vs Fc/Fc^+ .

The first three reductions of fullerene, Py_2C_{60} , are located at -1.12 , -1.50 , and -2.04 V vs Fc/Fc^+ (see Figure S4b in the Supporting Information). Upon forming $1\cdot\text{Py}_2\text{C}_{60}$ by equimolar addition of **1** to the solution of Py_2C_{60} , an additional reduction process occurred corresponding to the fulleropyrrolidine entity (see Figure 4b). The reduction potentials of the fullerene and ZnP entities revealed a small (~ 20 mV) potential shift upon axial coordination. The electrochemically evaluated HOMO(ZnP)–LUMO(Py_2C_{60}) gap for $1\cdot\text{Py}_2\text{C}_{60}$ was found to be ~ 1.40 V.

Anion binding to OxP is expected to exhibit large cathodic shifts of the oxidation potentials since the binding site is contained within the extended π -conjugated system. For example, F^- binding to OxP(bz)₂ exhibited a cathodic shift of nearly 600 mV for the first oxidation process²⁹ (see Figure S5 in the Supporting Information). Similar potential shifts were observed for other strongly binding anions; however, weakly binding anions such as ClO_4^- caused no substantial potential shifts.²⁹ This seems also to be the case when strongly interacting anions bind to the **1**·Py₂C₆₀ complex, as shown in Figure 4c. The OxP oxidation peak of the **1**·Py₂C₆₀ complex located at 0.48 V, although irreversible, anodically shifted by over 600 mV upon binding to F^- . It is important to note that, in the presence of F^- , the redox potentials of both ZnP and C₆₀ do not show significant changes, once again indicating no direct interaction of these entities with the anions. Similar voltammetric behavior was observed for strongly interacting acetate and dihydrogen phosphate anions but not for the weakly interacting perchlorate anions. The easier oxidation of strongly interacting anion-bound OxP compared to ZnP suggests that it acts as a terminal electron donor in the supramolecular complex, **1**(F^-)·Py₂C₆₀, affording the final CS state via photoinduced electron transfer from singlet excited porphyrinatozinc (1ZnP*) to the coordinated fullerene electron acceptor (Py₂C₆₀), followed by electron transfer from **1**(F^-) to ZnP⁺.

Steady-State Fluorescence Studies. The ZnP utilized in the construction of **1** emits at 613 and 667 nm, while the OxP entity shows a broad emission with a peak maximum at 724 nm. Owing to the presence of electron-deficient OxP, the emission bands of **1** are quenched substantially, as shown in Figure 5a.²³ The ZnP emission bands appear as shoulder bands to the OxP emission bands. The fluorescence spectrum of **1** revealed additional quenching upon addition of Py₂C₆₀ to form **1**·Py₂C₆₀, as shown in Figure 5a. Interestingly, addition of F^- to the **1**·Py₂C₆₀ solution resulted in little or no change in the peaks corresponding to both ZnP and OxP entities, as shown in Figure 5b. Based on energy calculations, quenching in **1**·Py₂C₆₀ could be attributed to photoinduced electron transfer from singlet excited ZnP to coordinated fullerene (*vide infra*). Further, time-resolved emission and transient absorption spectral studies were performed to unravel the quenching mechanism and effect of F^- on kinetics of electron transfer in the supramolecular complex.

Femtosecond Laser Flash Photolysis of the Supramolecular Complex between **1 and Py₂C₆₀.** Femtosecond transient absorption spectroscopy of the supramolecular complex (**1**(F^-)·Py₂C₆₀) with excitation at 440 nm reveals the transient absorption band at 900 nm due to the singlet excited state of the ZnP moiety of the supramolecular complex with the bleaching of the Q-band of the ZnP moiety at 600 nm as shown in Figure 6a. To our surprise, the transient absorption disappears completely at 100 ps, and the lifetime of the singlet excited state is determined to be 34 ps by the single-exponential curve fitting in Figure 6b. No triplet absorption due to ZnP or Py₂C₆₀ was observed. Under the experimental conditions of Figure 6, the concentration of **1**, Py₂C₆₀, and F^- is 1.5×10^{-4} M when 97% of each component forms the supramolecular complex, judging from the *K* value in Table 1 (1.9×10^5 M⁻¹). This is consistent with the fast decay of the singlet excited state of the ZnP moiety (¹ZnP*) in the supramolecular complex because there would be a long-lived component of the

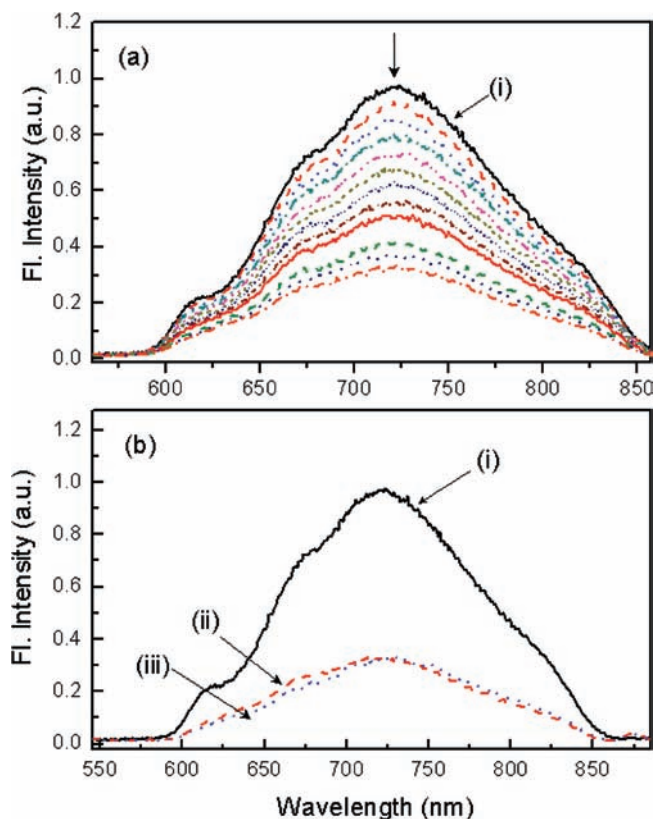


Figure 5. Steady-state fluorescence spectrum of **1** (a) on increasing addition of Py₂C₆₀ to form the **1**·Py₂C₆₀ complex (1.1 equiv total) and (b) on addition of F^- (1.1 equiv total) to the solution of **1**·Py₂C₆₀ to form the **1**(F^-)·Py₂C₆₀ complex in *o*-dichlorobenzene. The samples were excited at 440 nm, corresponding to ZnP Soret band, and the initial concentration of **1** was held at 50 μ M. Spectrum (i) represents that of **1** in the absence of guest entities, (ii) represents that of the **1**·Py₂C₆₀ complex, and (iii) represents that of the **1**(F^-)·Py₂C₆₀ complex.

singlet excited state of the ZnP moiety of free **1** molecules ($\tau = 1.9$ ns for ZnP)²³ if free **1** molecules remaining in solution were excited. The fast decay of ¹ZnP* may result from the fast electron transfer from ¹ZnP* to Py₂C₆₀ in the supramolecular complex. The absence of the absorption at 1000 nm due to Py₂C₆₀^{•-} in the transient absorption spectra suggests that back electron transfer from Py₂C₆₀^{•-} to ZnP⁺ to the ground state is much faster than the forward electron transfer. In such a case, the rate constant of electron transfer from ¹ZnP* to Py₂C₆₀ in the supramolecular complex to produce the CS state (*k*_{CS}) is determined to be 2.9×10^{10} s⁻¹ from the single-exponential curve fitting in Figure 6b.

Similar results were obtained for the supramolecular complexes with binding of different anions. Figure 7a shows the transient absorption spectra of the supramolecular complex with binding of acetate ion. The *k*_{CS} value is determined to be 1.2×10^{10} s⁻¹ from the single-exponential curve fitting in Figure 7b. This value is smaller than the value obtained for F^- binding. The *k*_{CS} values determined for other anions are listed in Table 1 (see Supporting Information for the transient absorption data). The *k*_{CS} values decrease in the order 2.9×10^{10} (F^-) > 1.5×10^{10} ($H_2PO_4^-$) > 1.2×10^{10} (CH_3COO^-) > 1.2×10^9 (ClO_4^-) > 6.3×10^8 (none) s⁻¹. Generally, the stronger the binding, the faster the electron-transfer rates.

CS State of the Supramolecular Complex between **1 and Py₂C₆₀ Detected by Nanosecond Laser Flash Photolysis.** In contrast to the case of femtosecond laser flash photolysis in Figure 6a, nanosecond transient absorption spectroscopy of

(29) Schumacher, A. L.; Hill, J. P.; Ariga, K.; D'Souza, F. *Electrochem. Commun.* **2007**, *9*, 2751.

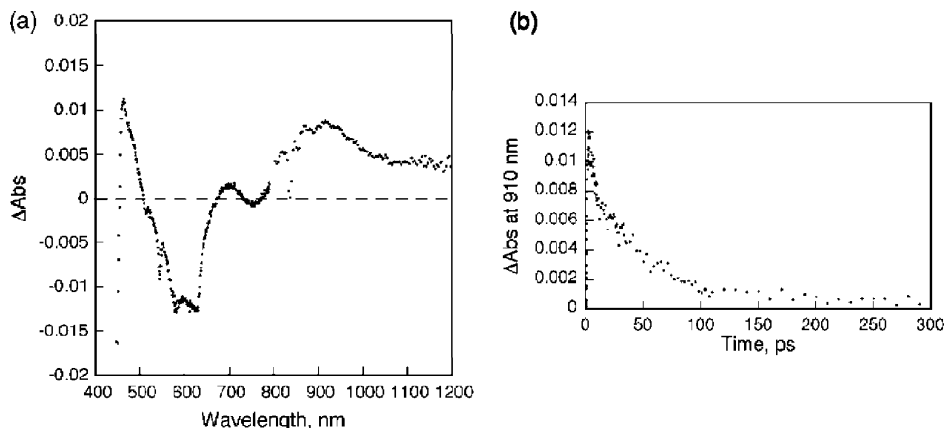


Figure 6. (a) Transient absorption spectrum of $\mathbf{1}(\text{F}^-)\cdot\text{Py}_2\text{C}_{60}$ in *o*-dichlorobenzene (concentration of each component, 1.5×10^{-4} M) at 2 ps after femtosecond laser excitation at 440 nm. (b) Decay of absorbance at 910 nm corresponding to the singlet excited state of the ZnP moiety in the supramolecular complex.

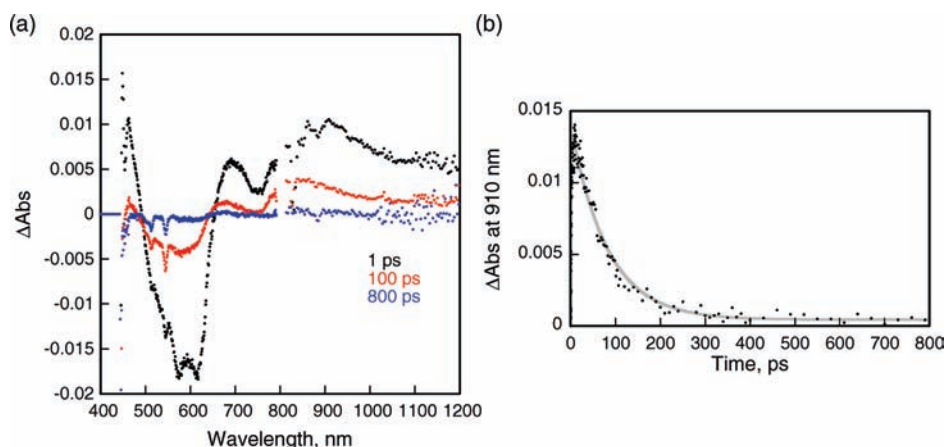


Figure 7. (a) Transient absorption spectra of $\mathbf{1}(\text{CH}_3\text{COO}^-)\cdot\text{Py}_2\text{C}_{60}$ in *o*-dichlorobenzene (concentration of each component, 1.5×10^{-4} M) at 1 (black), 100 (red), and 800 ps (blue) after femtosecond laser excitation at 440 nm. (b) Decay of absorbance at 910 nm corresponding to the singlet excited state of the ZnP moiety in the supramolecular complex.

$\mathbf{1}(\text{F}^-)\cdot\text{Py}_2\text{C}_{60}$ with excitation at 450 nm (Figure 8a) revealed the absorption band due to the fulleropyrrolidine anion radical at 1000 nm together with a broad absorption in the region of 700–800 nm. The absorption band at 700 nm is assigned to the triplet excited state of Py_2C_{60} .³⁰ The additional broad absorption band may be assigned to the radical cation of $\mathbf{1}(\text{F}^-)$.²⁵ This indicates the presence of a CS species, while kinetic measurements performed by monitoring the decay of the fullerene anion radical at 1000 nm give a surprisingly long lifetime for this species (14 μs), as shown in Figure 8b.

Since the singlet excited state ($^1\text{ZnP}^*$) in the supramolecular complex decays completely at 100 ps, as shown in Figure 6b, the triplet excited state ($^3\text{ZnP}^*$) rather than $^1\text{ZnP}^*$ should be involved for the formation of the CS state. Under the experimental conditions of Figure 8, the concentration of each component ($\mathbf{1}$, Py_2C_{60} , and F^-) is 3.0×10^{-5} M, which is smaller than that employed for the femtosecond laser flash photolysis, because a 1 cm path length cell was used for the nanosecond laser flash photolysis, whereas a 2 mm cell was used for the femtosecond laser flash photolysis. In such a case, 15% of the molecules of each component remain uncomplexed and the ZnP moiety of the free molecules is excited with nanosecond laser

excitation at 450 nm to produce $^3\text{ZnP}^*$ via intersystem crossing from $^1\text{ZnP}^*$ at the microsecond time scale in Figure 8. Then, intermolecular electron transfer from $^3\text{ZnP}^*$ to Py_2C_{60} may occur to afford the triplet supramolecular CS state. The dynamics of electron transfer from $^3\text{ZnP}^*$ to Py_2C_{60} are too fast to be monitored by nanosecond laser flash photolysis (inset of Figure 8b). On the other hand, the process of electron transfer from ZnP to $^3\text{Py}_2\text{C}_{60}^*$ could be observed as shown in the inset of Figure 8b. The $^3\text{C}_{60}^*$ is generated via energy transfer from $^1\text{ZnP}^*$ to C_{60} and intersystem crossing. The intermolecular second-order rate constant of electron transfer from ZnP to $^3\text{C}_{60}^*$ was determined to be $(1.5 \pm 0.3) \times 10^{10} \text{ M}^{-1} \text{ s}^{-1}$ from the rise of absorbance at 1000 nm due to C_{60}^* .

The single-exponential decay of the CS state (Figure 8b) indicates the formation of the supramolecular complex following the intermolecular photoinduced electron-transfer reaction. When the concentration of $\mathbf{1}(\text{F}^-)\cdot\text{Py}_2\text{C}_{60}$ was decreased, the quantum yield of the CS state [$\Phi(\text{CS})$], determined using a comparative method,³³ increased to 0.14 ± 0.02 at 3.0×10^{-5} M of equimolar $\mathbf{1}(\text{F}^-)$ and Py_2C_{60} , as shown in Figure 9. The observed quantum yields depending on concentration of equimolar $\mathbf{1}(\text{F}^-)$ and Py_2C_{60} agreed with the ratio of the uncomplexed porphyrin component determined from the formation constant of the supramolecular complex ($K = 1.9 \times 10^5 \text{ M}^{-1}$ in Table 1). The observed long lifetime of the CS state may be a consequence

(30) Guldi, D. M.; Kamat, P. V. In *Fullerenes: Chemistry, Physics and Technology*; Kadish, K. M., Ruoff, R. S., Eds.; Wiley Interscience: New York, 2000.

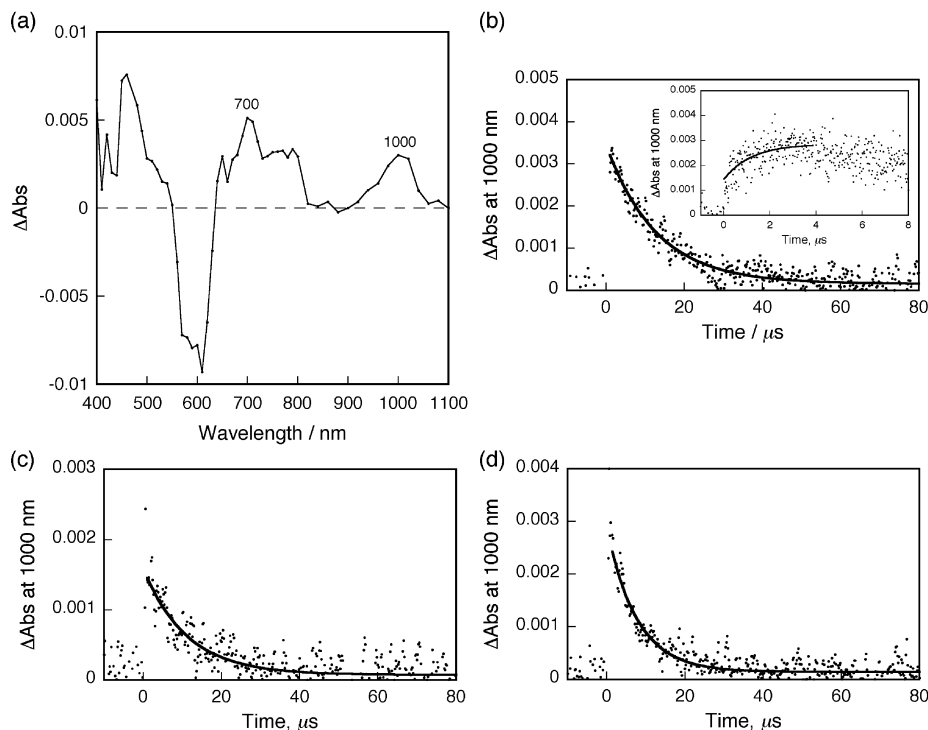


Figure 8. (a) Transient absorption spectrum of $1(F^-) \cdot Py_2C_{60}$ in *o*-dichlorobenzene (concentration of each component, 3.0×10^{-5} M) at $1 \mu s$ after nanosecond laser excitation at 450 nm. (b) Decay of absorbance for $1(F^-) \cdot Py_2C_{60}$ at 1000 nm, corresponding to fullerene anion radical. Inset: 0–8 μs time range. (c) Decay of absorbance for $1(CH_3COO^-) \cdot Py_2C_{60}$ at 1000 nm. (d) Decay of absorbance for $1(H_2PO_4^-) \cdot Py_2C_{60}$ at 1000 nm.

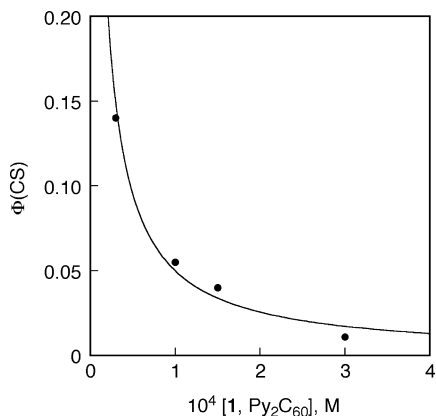


Figure 9. Plot of the quantum yield of the CS state of $1(F^-) \cdot Py_2C_{60}$ [$\Phi(CS)$] vs concentration of equimolar **1** and Py_2C_{60} with tetra-*n*-butylammonium fluoride (1.0×10^{-3} M) in *o*-dichlorobenzene. The solid line represents the ratio of uncomplexed ZnP calculated using $K = 1.9 \times 10^5 M^{-1}$.

of the persistence of the triplet-correlated radical-ion-pair character in the CS state, which results in the corresponding forbidden charge recombination back to the singlet ground state in contrast to the case of the singlet CS state in Figure 6. The triplet multiplicity of the CS state, which is populated by the intermolecular electron transfer from ${}^3ZnP^*$ to Py_2C_{60} or from ZnP to ${}^3Py_2C_{60}^*$, plays a crucial role in determining its very long lifetime of 14 μs . The spin conversion from the triplet supramolecular CS state to the singlet CS state may be prohibited because of the short distance between the radical ions in the supramolecular complex, which results in a large

magnitude of the spin exchange interaction (J).^{31,32} Additionally, we have examined nanosecond laser flash experiments in the presence of O_2 to estimate the spin state of the CS state. No transient absorption due to the CS state of $1(F^-) \cdot Py_2C_{60}$ was observed in aerated *o*-dichlorobenzene. The CS state was efficiently quenched by O_2 via energy transfer since electron transfer from $C_{60}^{\cdot-}$ of the CS state would be relatively slow.³⁴ This confirms that the long-lived CS state is a triplet radical ion pair.

The triplet supramolecular CS lifetime decreases with weaker binding of anions, as indicated by the decay time profile of absorbance at 1000 nm for $1(CH_3COO^-) \cdot Py_2C_{60}$ (11 μs) and $1(H_2PO_4^-) \cdot Py_2C_{60}$ (7.5 μs) in Figure 8c and d, respectively. In the case of ClO_4^- , no anion binding was observed when the CS lifetime (0.17 μs) was the same as that without anion (0.16 μs). Thus, the introduction of the fluoride cofactor into the $1 \cdot Py_2C_{60}$ complex results in an ~ 90 -fold enhancement of the lifetime of the CS species over that of the noncomplexed $1 \cdot Py_2C_{60}$.

- (31) (a) Mori, Y.; Sakaguchi, Y.; Hayashi, H. *J. Phys. Chem. A* **2002**, *106*, 4453. (b) Wegner, M.; Fischer, H.; Grosse, S.; Vieth, H.-M.; Oliver, A. M.; Paddon-Row, M. N. *Chem. Phys.* **2001**, *264*, 341.
- (32) The magnitude of J of electron donor–acceptor dyads with little interaction is normally much smaller (typically $|J| < 10^{-2}$ kJ mol⁻¹) than the thermal energy at ambient temperature. See: (a) Kobori, Y.; Yamauchi, S.; Akiyama, K.; Tero-Kubota, S.; Imahori, H.; Fukuzumi, S.; Norris, J. R., Jr. *Proc. Natl. Acad. Sci. U.S.A.* **2005**, *102*, 10017. (b) Kobori, Y.; Shibano, Y.; Endo, T.; Tsuji, H.; Murai, H.; Tamao, K. *J. Am. Chem. Soc.* **2009**, *131*, 1624.
- (33) Ohkubo, K.; Shao, J.; Ou, Z.; Kadish, K. M.; Li, G.; Pandey, R. K.; Fujitsuka, M.; Ito, O.; Imahori, H.; Fukuzumi, S. *Angew. Chem., Int. Ed.* **2004**, *43*, 853.
- (34) Nakanishi, I.; Fukuzumi, S.; Konishi, T.; Ohkubo, K.; Fujitsuka, M.; Ito, O.; Miyata, N. *J. Phys. Chem. B* **2002**, *106*, 2372.

In the absence of F^- , excitation of the porphyrinatozinc results primarily in charge separation, leading to the formation of $ZnP^{*+}-C_{60}^{-}$ (energy 1.40 eV), which persists for a few hundred nanoseconds before relaxing to the ground state. Complexation of F^- to the OxP center lowers its oxidation potential by nearly 600 mV²⁵ (see Figure 4), thus creating an intermediate energy state for charge migration from the ZnP^{*+} to the $F^-:OxP$ center (energy < 0.83 eV). The increase in the reorganization energy of electron transfer combined with the decrease in CR driving force caused by F^- binding results in a reduction in the rate of the CR process and an increase in the lifetime of the triplet supramolecular CS state.

Conclusions

In summary, we have observed the first example of anion-complexation-induced enhancement of the charge separation in a supramolecular complex to produce the singlet CS states and also stabilization of the triplet CS states in an oligochromophoric molecule possessing exclusive binding sites for both a guest electron acceptor and an anionic cofactor species. This work not only illustrates a novel method for controlling the persistence of CS states but also demonstrates the great utility of the supramolecular assembly route to give complex functional systems. Finally, it is important to note the indispensability of the oxoporphyrinogen framework in this system, since it allows for the selective positioning of substituents by virtue of its

special reactivity toward alkylating reagents and permits electrochemical control of its redox potentials in the presence of inorganic anions.

Acknowledgment. This research was supported by a Grant-in-Aid for Scientific Research on Priority Area "Super-Hierarchical Structures" at the World Premier International Research Center Initiative (WPI Initiative) on Materials Nanoarchitectonics (to J.P.H.), KOSEF/MEST through WCU project (R31-2008-000-10010-0), and a Global COE program "Global Education and Research Center for Bio-Environmental Chemistry" (to S.F.) from the Ministry of Education, Culture, Sports, Science and Technology, Japan, and also by the National Science Foundation (0804015 to F.D.). Y.X. thanks the Shanghai Pujiang Program (08PJ14037), China.

Supporting Information Available: Optical absorption spectral changes observed during binding of acetate, dihydrogen phosphate, and perchlorate to $\mathbf{1}\cdot Py_2C_{60}$ in *o*-dichlorobenzene; cyclic voltammograms of OxP(bz)₂, Py₂C₆₀, and OxP(bz)₂ in the presence of various amounts of F^- ; femtosecond transient absorption spectra of $\mathbf{1}(H_2PO_4)\cdot Py_2C_{60}$ in dichlorobenzene. This information is available free of charge via the Internet at <http://pubs.acs.org>.

JA9048306